

Amyloid β -Protein Assembly: Differential Effects of the Protective A2T Mutation and Recessive A2V Familial Alzheimer's Disease Mutation

Xueyun Zheng,[†] Deyu Liu,[†] Robin Roychaudhuri,[‡] David B. Teplow,[‡] and Michael T. Bowers^{*,†}

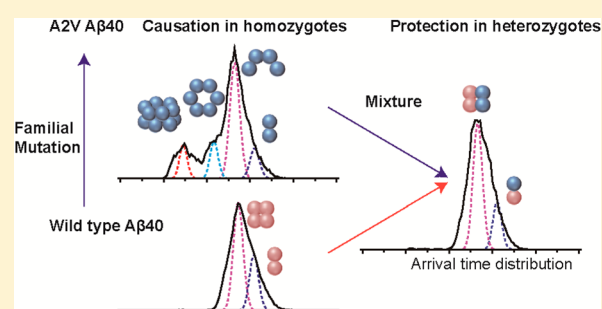
[†]Department of Chemistry and Biochemistry, University of California, Santa Barbara, California 93106, United States

[‡]Department of Neurology, David Geffen School of Medicine, Molecular Biology Institute and Brain Research Institute, University of California Los Angeles, Los Angeles, California 90095, United States

S Supporting Information

ABSTRACT: Oligomeric states of the amyloid β -protein ($A\beta$) appear to be causally related to Alzheimer's disease (AD). Recently, two familial mutations in the amyloid precursor protein gene have been described, both resulting in amino acid substitutions at Ala2 (A2) within $A\beta$. An A2V mutation causes autosomal recessive early onset AD. Interestingly, heterozygotes enjoy some protection against development of the disease. An A2T substitution protects against AD and age-related cognitive decline in non-AD patients. Here, we use ion mobility-mass spectrometry (IM-MS) to examine the effects of these mutations on $A\beta$ assembly. These studies reveal different assembly pathways for early oligomer formation for each peptide. A2T $A\beta$ 42 formed dimers, tetramers, and hexamers, but dodecamer formation was inhibited. In contrast, no significant effects on $A\beta$ 40 assembly were observed. A2V $A\beta$ 42 also formed dimers, tetramers, and hexamers, but it did not form dodecamers. However, A2V $A\beta$ 42 formed trimers, unlike A2T or wild-type (wt) $A\beta$ 42. In addition, the A2V substitution caused $A\beta$ 40 to oligomerize similar to that of wt $A\beta$ 42, as evidenced by the formation of dimers, tetramers, hexamers, and dodecamers. In contrast, wt $A\beta$ 40 formed only dimers and tetramers. These results provide a basis for understanding how these two mutations lead to, or protect against, AD. They also suggest that the $A\beta$ N-terminus, in addition to the oft discussed central hydrophobic cluster and C-terminus, can play a key role in controlling disease susceptibility.

KEYWORDS: Amyloid β -protein, familial Alzheimer's disease, A2T, A2V, oligomerization, ion mobility spectrometry, mass spectrometry



Amyloid β -protein ($A\beta$) plays an important role in Alzheimer's disease (AD) pathogenesis.^{1,2} $A\beta$ is produced from amyloid precursor protein (APP) by successive endoproteolytic cleavages by β - and γ -secretase. $A\beta$ exists in the body primarily in two forms, 40- ($A\beta$ 40) or 42-residues ($A\beta$ 42) in length. Although $A\beta$ 40 is present in the body at a concentration \approx 10-fold that of $A\beta$ 42, the latter peptide is more toxic and is the primary component of amyloid plaques.³ Although pathognomonic for AD, fibril-containing plaques do not appear to be the primary pathologic agents in AD: the primacy of $A\beta$ oligomers has been suggested instead.^{4,5} In solution, $A\beta$ 40 and $A\beta$ 42 monomers are both intrinsically disordered, yet they display distinct aggregation pathways on the way to fibril formation. $A\beta$ 40 initially forms small oligomers, including dimers and tetramers, whereas $A\beta$ 42 forms larger aggregates, including dimers, tetramers, hexamers, and dodecamers. These oligomeric states appear to be on-pathway for fibril formation.^{6,7} Of these oligomers, the 56 kDa dodecamer has been shown to be a proximate toxic agent for AD pathology.^{8,9}

Although most AD cases occur sporadically, \sim 5% of AD cases are caused by mutations in the APP,^{10,11} presenilin 1 (PS1),^{12,13} or presenilin 2 (PS2)¹⁴ genes. These familial AD (FAD) cases often lead to early onset of disease ($<$ 60 years of age). Numerous FAD-related mutations in the APP gene have been identified, and many of them are near β - or γ -secretase cleavage sites. This results most commonly in overproduction of $A\beta$ or increases in the amount of $A\beta$ 42 that is produced relative to $A\beta$ 40.¹⁵ However, as many mutations occur within the $A\beta$ region, it is very likely that these substitutions would alter the structural and aggregation properties of the resultant $A\beta$ 42 and $A\beta$ 40 peptides. Notably, many mutations in the APP gene result in amino acid substitutions within the central region of $A\beta$, such as, for example, Flemish (A21G),¹⁶ Arctic (E22G),¹⁷ Dutch (E22Q),¹⁸ Osaka (E22 Δ),¹⁹ Italian (E22K),²⁰ and D23N (Iowa)²¹ mutations. The resulting peptides exhibit distinct aggregation propensities and toxicities.

Received: June 22, 2015

Revised: August 2, 2015

Published: August 5, 2015

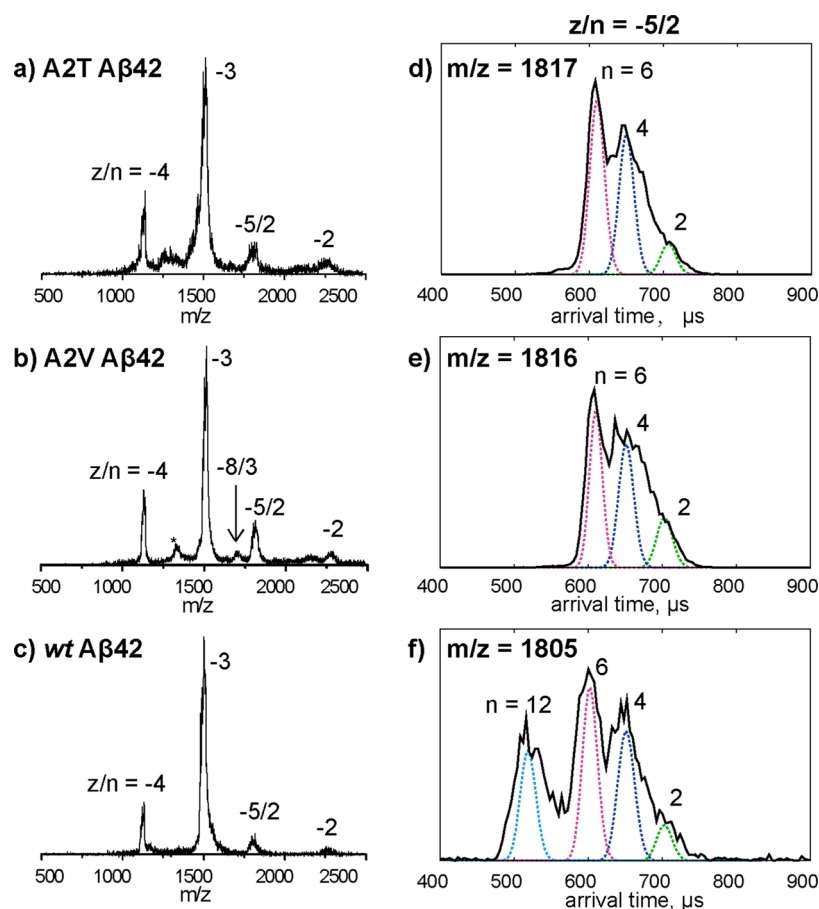


Figure 1. (a–c) Mass spectra of A2T, A2V, and wt Aβ42. The charge state of each species is noted with z/n , where z is the charge and n is oligomer number. The peak marked with an asterisk (*) in panel b is assigned as a fragment peak or impurity (see discussion in the [Supporting Information](#)). (d–f) ATDs of $z/n = -5/2$ peaks for A2T, A2V, and wt Aβ42. The oligomer order (n) is noted for each feature. The dashed lines represent the peak shape for a single conformation. Injection energy studies of the $z/n = -5/2$ A2T and A2V Aβ42 peaks are provided in [Figure S1](#). The injection energy in panels d–f is 40 eV.

The central region of Aβ has been shown to be crucial for the initial nucleation of Aβ folding and assembly.²² Mutations near this region may disrupt the conformation of Aβ, resulting in increased aggregation propensity and formation of toxic oligomers.²³ On the other hand, the role of the N-terminus in aggregation, toxicity, and pathology has been less thoroughly studied due to the fact that this region appears to be disordered in the fibril state.^{24,25} However, as with the central region of Aβ, a number of APP mutations result in amino acid substitutions at the N-terminus, and these substitutions alter Aβ assembly. These include the English (H6R),^{26,27} Tottori (D7N),^{26–29} and Taiwanese (D7H)³⁰ mutations. The importance of the Aβ N-terminus in disease causation thus is clear. Most recently, two new APP mutations have been described that result in the substitutions A2T and A2V can be important in Aβ structure and assembly.^{31,32} In the work presented here, we elucidate the effects on early Aβ assembly of these two recently discovered mutations.

The A2T substitution substantially decreases AD risk as well as protects against age-related cognitive decline in the elderly without AD.³¹ It is thought to be the first example of a sequence variant that protects against AD. The A2T substitution occurs immediately adjacent to the β-secretase site, and, indeed, the mutation has been found to reduce Aβ production ~20% in heterozygous carriers. Such a reduction may be responsible for its protective function in AD

pathology.³¹ However, as the mutation is within the Aβ sequence, it is possible that the A2T mutation also changes the aggregation properties of Aβ proteins, thus contributing to its protective effect, a possibility that we investigate here.

The mutation causing the A2V substitution results in early onset AD in homozygotes, whereas some protection against AD is observed in heterozygotes.³² In contrast to the A2T substitution, A2V increases Aβ production. Interestingly, coincubation of A2V Aβ42 and wt Aβ42 produced slower aggregation rates than those exhibited by either peptide alone, as well as decreased toxicity.³² The A2V substitution accelerates Aβ42 oligomerization and also leads to the production of annular structures with a higher hydrophobicity than that of wt Aβ42.³³

A consensus regarding the effects of the A2T and A2V substitutions on Aβ assembly has not been reached. Two recent studies of A2T and A2V peptides reported different aggregation kinetics by thioflavin T (ThT) fluorescence studies. Benilova et al. showed that the A2T substitution has little effect on Aβ42 aggregation, but it did affect its solubility.³⁴ Maloney et al., in contrast, showed that the A2T mutant had a lower aggregation propensity compared to that of the A2V mutant or wt Aβ42.³⁵ For Aβ40, the A2T mutant was shown to aggregate similarly to wt, whereas the A2V mutant exhibited faster aggregation and a shorter lag phase, making this peptide behave more Aβ42-like.^{34,35}

To improve our understanding of the A2T and A2V substitutions, we used ion mobility coupled to mass spectrometry (IM-MS) to examine the early assembly and subsequent aggregation of these mutant peptides. IM-MS can separate species with the same mass-to-charge (m/z) ratio but different shapes or sizes.³⁶ As a consequence, it has successfully revealed the structures on $A\beta$ oligomers and the effects of small molecule inhibitors of $A\beta$ assembly.^{7,29,37–42} We examine here the early oligomer distributions of A2T- and A2V-containing $A\beta$ 40 and $A\beta$ 42 to understand how each assembles and whether the early assembly pathways are identical or different. We also examine the early oligomer distributions of mixtures of wt and mutant peptides to understand how each affects the other's assembly. This provides the means to model *in vitro* the homozygous and heterozygous states that exist in humans. These studies provide mechanistic insights into the etiology of FAD, mechanisms of protection from FAD, and potential targets for therapeutic agents.

RESULTS

Different Oligomer Distributions of wt and Mutant $A\beta$ 42. Mass spectra of wt $A\beta$ 42, A2T, and A2V were recorded individually and are shown in Figure 1a–c. Four common peaks were observed for each peptide, corresponding to z/n ratios of -4 , -3 , $-5/2$ and -2 , where z is charge and n is oligomer size. The mass spectrum of A2V $A\beta$ 42 was interesting because, in addition to the four peaks, another peak was observed between $z/n = -3$ and $-5/2$ in the spectrum, corresponding to $z/n = -8/3$. This indicates the A2V mutant forms a trimer, which is not observed for wt or A2T $A\beta$ 42. Moreover, there is another peak between $z/n = -4$ and -3 for A2V, denoted by an asterisk (*), which is assigned as a fragment peak or impurity (see Supporting Information, Figure S3, for a detailed discussion of this peak assignment).

The arrival time distributions (ATDs) of the $z/n = -5/2$ peaks for all three $A\beta$ 42 alloforms are shown in Figure 1d,e. The ATD of wt $A\beta$ 42 shows four features, with arrival times at ~ 710 , 670 , 610 , and $540 \mu\text{s}$, which were previously assigned as $A\beta$ 42 dimer, tetramer, hexamer, and dodecamer, respectively, based on their collision cross sections (see ref 7 for a detailed discussion of these assignments). However, the ATD of A2T or A2V $A\beta$ 42 (Figure 1d or e) shows only three features, with arrival times at ~ 710 , 670 , $610 \mu\text{s}$, which were assigned as dimer, tetramer, and hexamer, respectively, based on their cross sections. There is no feature at lower arrival time observed in either of the ATD for mutants, indicating that no other oligomers larger than hexamers are formed. These results suggest the formation of $A\beta$ 42 dodecamer is inhibited by both A2T and A2V mutations.

To assign the peaks in the ATDs unambiguously, and to better understand the oligomer distributions of the $A\beta$ 42 mutants, the $-5/2$ ATDs for $A\beta$ 42 mutants were measured at different injection energies. At low injection energy, the ions are rapidly thermalized by cooling collisions with the helium gas in the drift cell and therefore large complexes can be preserved through the process. At high injection energy, the ions are given sufficient energy to lead to internal excitation, which can cause isomerization into a low energy structure or dissociation of large noncovalent complexes into smaller species. As shown in Figure S1, the ATDs measured at intermediate injection energy (40 eV) are the same ones shown in Figure 1d,e. When the injection energy is lowered to 25 eV (Figure S1 top panel), the hexamer peak becomes especially prominent, whereas the

tetramer and dimer features decrease. However, there are still no peaks with earlier arrival times observed, suggesting that oligomers of size dodecamer or larger are not formed in solution. At high injection energy (100 eV, Figure S1, bottom panel), the hexamer peak disappears, whereas the tetramer and dimer peaks dominate the spectrum. This suggests hexamer dissociation into smaller oligomers. These injection energy studies are fully consistent with the assignment of the three peaks in the ATDs as dimer, tetramer, and hexamer.

Ion Mobility Study of $z/n = -2$ and $-8/3$ Peaks: A2V $A\beta$ 42 Forms Trimers. The $z/n = -2$ $A\beta$ 42 is a relative low charge state of the $A\beta$ 42 alloforms and possibly consists of high order oligomers, making its ATD of interest. The signal of the $z/n = -2$ peak for wt $A\beta$ 42 is too low to obtain a reliable ATD; therefore, no data for it is shown. However, we were able to record ATDs for the -2 peaks of A2T and A2V $A\beta$ 42 (Figure 2).

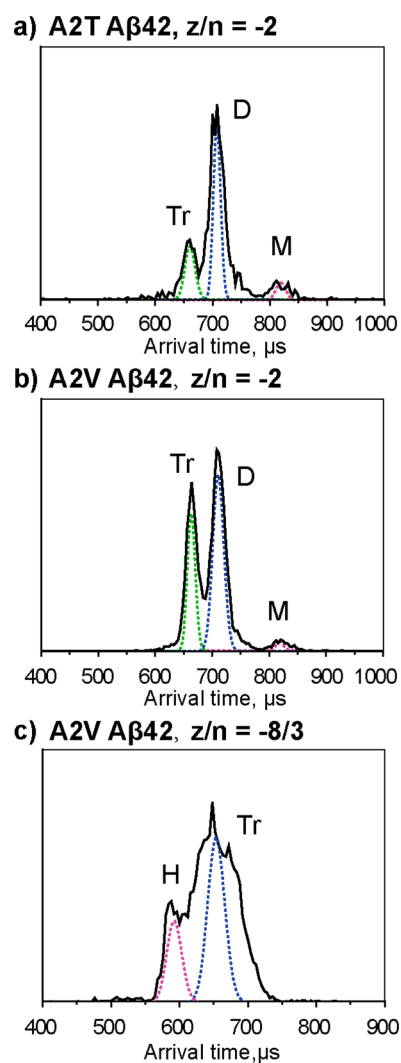


Figure 2. (a, b) ATDs of the $z/n = -2$ peaks for A2T and A2V $A\beta$ 42, respectively. (c) ATD of the $z/n = -8/3$ peak for A2V. The dashed lines represent the peak shape for a single conformation. The oligomer order is noted for each feature, where M represents monomer, D represents dimer, Tr represents trimer, and H represents hexamer. The injection energy is 40 eV. Summary of ATDs for each peak and their cross sections for $A\beta$ 42 alloforms is given in Figure S7.

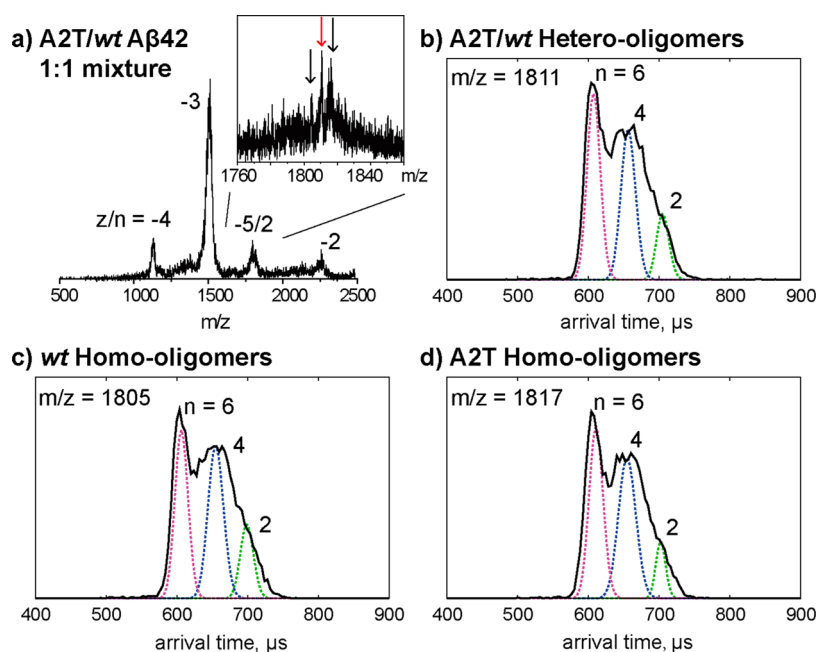


Figure 3. Ion mobility study of an equimolar mixture of wt and A2T Aβ42. (a) Full mass spectrum of a wt/A2T Aβ42 mixture and a zoomed-in spectrum of $z/n = -5/2$ peaks that contains three species, which correspond to wt Aβ42 homo-oligomers, wt/A2T Aβ42 hetero-oligomers, and A2T Aβ42 homo-oligomers. (b–d) ATDs of the three $-5/2$ oligomer peaks. The oligomer order (n) is noted for each feature. The dashed lines represent the peak shape for a single conformation. The injection energy in panels b–d is 40 eV.

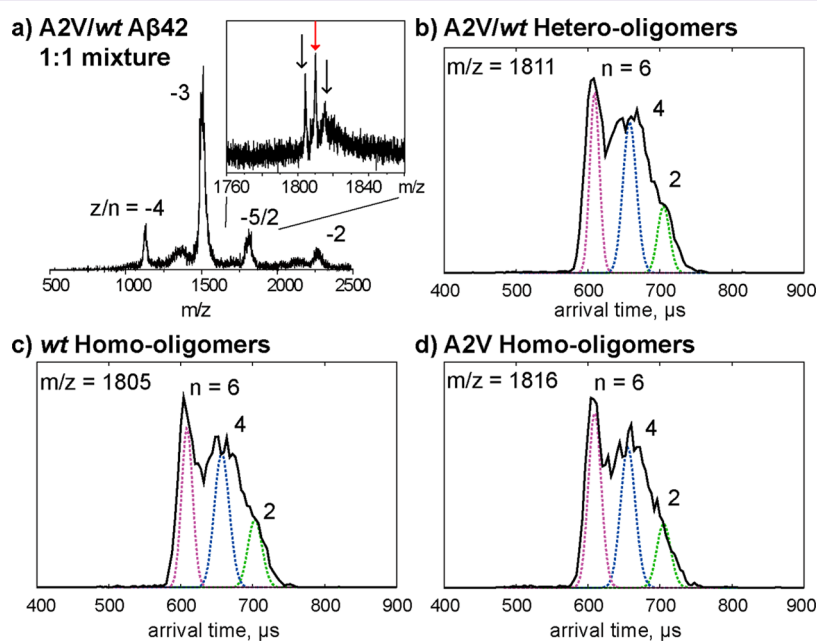


Figure 4. Ion mobility study of an equimolar mixture of wt Aβ42 and A2V mutant. (a) Full mass spectrum of A2V/wt Aβ42 mixture and a zoomed-in spectrum of $z/n = -5/2$ peaks that contains three species, which correspond to wt Aβ42 homo-oligomers, wt/A2V Aβ42 hetero-oligomers, and A2V Aβ42 homo-oligomers. (b–d) ATDs of the three $-5/2$ oligomer peaks. The oligomer order (n) is noted for each feature. The dashed lines represent the peak shape for a single conformation. The injection energy in panels b–d is 40 eV.

The ATD of -2 A2T Aβ42 shows three features, with arrival times at ~ 820 , 720 , 670 μs, which can be assigned as monomer, dimer, and trimer, respectively. Similarly, the ATD of the $z/n = -2$ A2V Aβ42 shows three features, corresponding to monomer, dimer, and trimer. However, the relative intensity of the A2T trimer is much lower than that of its dimer, whereas the relative intensity of the A2V trimer is comparable to that of its dimer, indicating that the formation of trimer is more favored for A2V Aβ42. Injection energy results (Figure S2b)

support this trend. At low injection energies, the trimer of A2V Aβ42 is dominant, whereas the trimer of A2T Aβ42 remains minor, indicating that trimer in the A2V mutant is significant in solution.

The ATD of $z/n = -8/3$ A2V Aβ42 shows two features, with arrival times at ~ 660 and 590 μs, which correspond to an A2V trimer and hexamer, respectively (Figure 3c). The breadth of the trimer feature indicates that there is a family of trimer structures existing in the solution. The injection energy study of

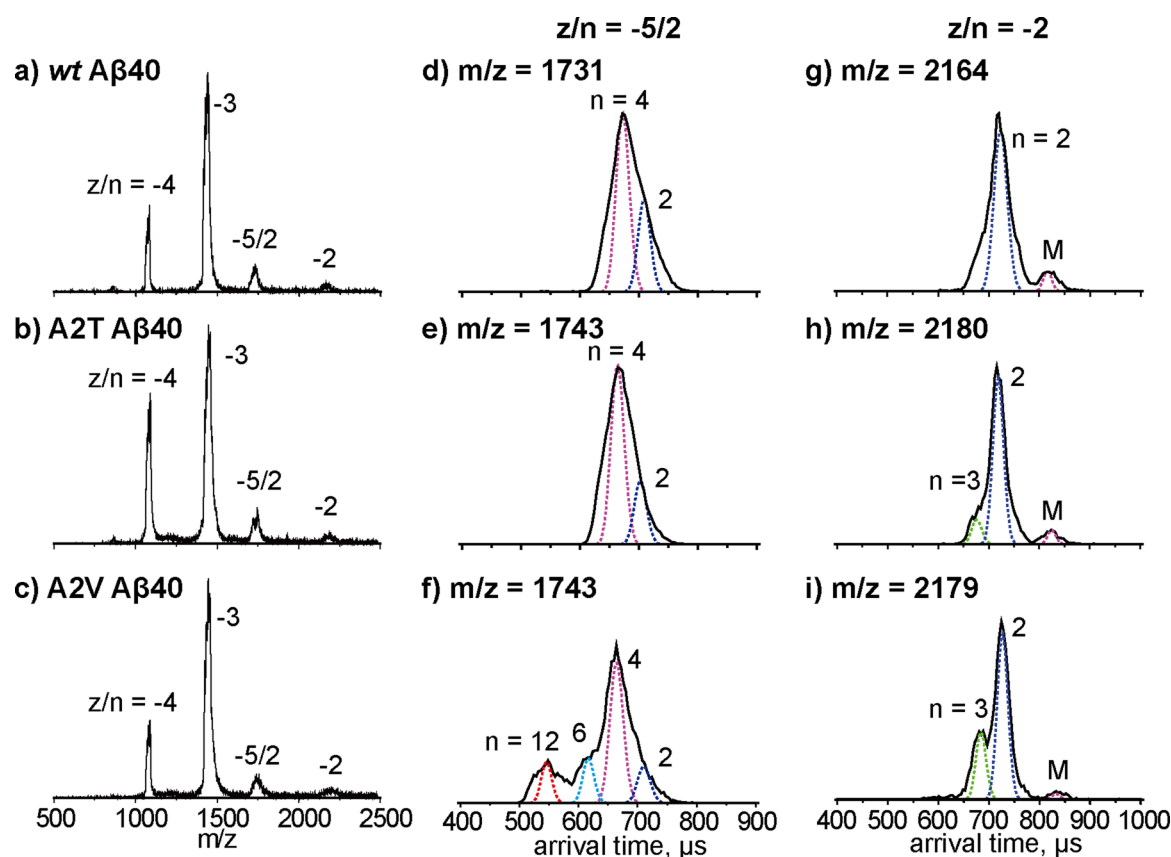


Figure 5. (a–c) Mass spectra of wt, A2T, and A2V Aβ40. The charge state of each species is noted with z/n , where z is the charge and n is oligomer number. (d–f) ATDs of $z/n = -5/2$ peaks for wt, A2T, and A2V Aβ40. (g–i) ATDs of $z/n = -2$ peaks for wt, A2T, and A2V Aβ40. The oligomer order (n) is noted for each feature. The dashed lines represent the peak shape for a single conformation. The injection energy in panels d–i is 40 eV. Summary of ATDs for each peak and their cross sections for Aβ40 alloforms is given in Figure S8.

–8/3 A2V Aβ42 (Figure S2c) indicates that the hexamer feature increases at lowest energies and the trimer peak gets sharper. At high energy (100 eV), the hexamer feature disappears and the broad trimer feature becomes the dominant peak.

Taken together, these ion mobility results reveal that the oligomerization pattern is different for each of the alloforms. wt Aβ42 forms dimer, tetramer, hexamer, and dodecamer. A2T and A2V Aβ42 form dimer, tetramer, and hexamer, without the formation of dodecamer, but A2V forms a significant trimer, which is only very minor in A2T and may not be present in wt Aβ42 at all.

Transmission electron microscopy (TEM) images were recorded for the same Aβ42 samples after 5 days of incubation at room temperature, and the results are shown in Figure S9. The wt Aβ42 forms long fibrils after 5 days of incubation, whereas A2T and A2V Aβ42 form some short fibrils or protofibrils along with some long fibrils. These results are consistent with those of a previous study³⁴ and suggest that the oligomers we detected are on-pathway.

Mixtures of wt and Mutant Aβ42: Effects on wt Aβ42 Oligomerization. The A2T mutation has been shown to protect carriers from AD or normal age-related cognitive decline.³¹ To model the effects of this peptide in heterozygotes, we created an equimolar mixture of A2T and wt Aβ42 and then performed MS (Figure 3). Four sets of peaks were observed, corresponding to $z/n = -4, -3, -5/2$, and -2 charge states. A zoomed-in spectrum of the $-5/2$ region using the QTOF-MS was obtained and shows that there are three peaks with charge

state of $-5/2$, which correspond to $-5/2$ wt Aβ42 homo-oligomers, wt/A2T hetero-oligomers (1:1 ratio), and A2T homo-oligomers. The ATDs of these three peaks (Figure 3b–d) display a similar oligomer distribution with three features, with arrival times of $\sim 710, 670$, and $600 \mu\text{s}$. We assign these features as dimers, tetramers, and hexamers, respectively. Note that no feature at shorter arrival time was observed, indicating that there is no homo/hetero-dodecamer or higher oligomer formation. These results indicate that the A2T mutant forms small hetero-oligomers (up to heterohexamers) with wt Aβ42 and inhibits the formation of wt Aβ42 dodecamer or higher oligomers.

Previous studies showed that A2V is a recessive mutation that causes early onset of AD in homozygotes but appears to be protective in heterozygotes.³² To provide an insight into this observation, we performed ion mobility studies on an equimolar mixture of wt and A2V Aβ42 (Figure 4). Similar to the A2T/wt mixture, the A2V/wt mixture shows three $-5/2$ peaks, corresponding to wt Aβ42 homo-oligomers, wt/A2V hetero-oligomers (1:1 ratio), and A2V homo-oligomers. The ATDs of these $-5/2$ peaks all show three features that can be assigned as dimer, tetramer, and hexamer, respectively. The data show that A2V Aβ42 forms small hetero-oligomers (only up to hexamers) with wt Aβ42 and prevents the formation of larger oligomers.

There is no $-8/3$ trimer peak observed in the equimolar mixture of wt and A2V Aβ42. Moreover, the ATD of the $z/n = -2$ peak for the wt/A2V mixture (Figure S4b) shows a dominant dimer peak and only a minor trimer peak, unlike that

of A2V alone (Figure 2b). These results indicate that A2V trimer formation is inhibited by wt A β 42.

Ion Mobility Study of A β 40 Mutants: A2V A β 40 Forms Hexamer and Dodecamer. We next examined the effects of the A2T and A2V substitutions on A β 40 assembly (see Figure 5). The mass spectra for the A2T and A2V mutants (Figure 5b,c) showed four peaks, corresponding to $z/n = -4, -3, -5/2$, and -2 , which is similar to that of wt A β 40 (Figure 5a).

The ATD of $z/n = -5/2$ wt A β 40 (Figure 5d) displays two features, with arrival times at ~ 710 and $670 \mu\text{s}$, which were previously assigned as A β 40 dimer and tetramer, respectively.⁷ The ATD of the $z/n = -5/2$ A2T A β 40 (Figure 5e) again shows two features, with arrival times at ~ 710 and $670 \mu\text{s}$, corresponding to dimer and tetramer, respectively. This ATD was similar to that of wt A β 40. However, the ATD of $z/n = -5/2$ A2V A β 40 (Figure 5f) shows four features, with arrival times of $\sim 710, 670, 620$, and $550 \mu\text{s}$, which can be assigned as dimer, tetramer, hexamer, and dodecamer, respectively. Hence, A2V A β 40 forms hexamers and dodecamers, something not observed for wt or A2T A β 40. This is consistent with previous ThT studies showing that A2V A β 40 displays a shorter lag phase during aggregation, which is similar to that of wt A β 42.^{34,35}

The ATDs of $z/n = -2$ A β 40 alloforms were recorded and are shown in Figure 5g–i. The ATD of wt A β 40 shows a dominant dimer peak at $\sim 720 \mu\text{s}$ and a small monomer peak at $\sim 840 \mu\text{s}$. The dimer peak is slightly broad at the bottom, which indicates that there might be a small amount of trimer formed. The ATDs of A2T and A2V A β 40 (Figure 5h,i) show one additional peak, with a shorter arrival time at $\sim 680 \mu\text{s}$, which is assigned as trimer. The relative intensity of the A2V trimer is greater than that of the A2T trimer or wt A β 40 trimer. This is consistent with the results of $z/n = -5/2$ peaks, which suggests that A2V A β 40 is aggregating into larger oligomers than are A2T and wt A β 40.

In summary, the A2T mutation does not significantly change A β 40 oligomerization. The A2V mutation, in contrast, promotes A β 40 oligomerization and causes it to undergo a more A β 42-like aggregation process. Although the relative intensity of the A2V dodecamer is smaller than that observed for wt A β 42 (Figure 1f), the A β 40 isoform is 10 times more abundant than A β 42 *in vivo*. Hence, this is a significant result and is fully consistent with the fact that homozygous carriers of the A2V mutation develop early onset AD.

The TEM results of A β 40 samples after 5 days of incubation (Figure S9) showed that they all formed short fibrils along with some annuli-like aggregates. Interestingly, the A β 40 A2V fibrils are thinner and tend to clump together to form plaques, indicating that the aggregation of A β 40 A2V is faster than that of wt or A2T A β 40.

The results of coincubation experiments using wt and mutant A β 40 are shown in Figures S5 and S6. The A2T/wt A β 40 mixture shows formation of homo/hetero-dimer and tetramer, which is similar to that of wt A β 40, indicating no enhancement of aggregation by A2T. Similarly, the A2V/wt mixture shows only homo- and heterodimer and tetramer. This is important because it indicates wt A β 40 inhibits formation of A2V hexamer or dodecamer. Hence, heterozygous A2V carriers are protected from dodecamer formation, whereas homozygous A2V carriers are not.

DISCUSSION

Our results show that amino acid substitutions at Ala2 of A β affect A β oligomerization (summarized in Figure 6). The

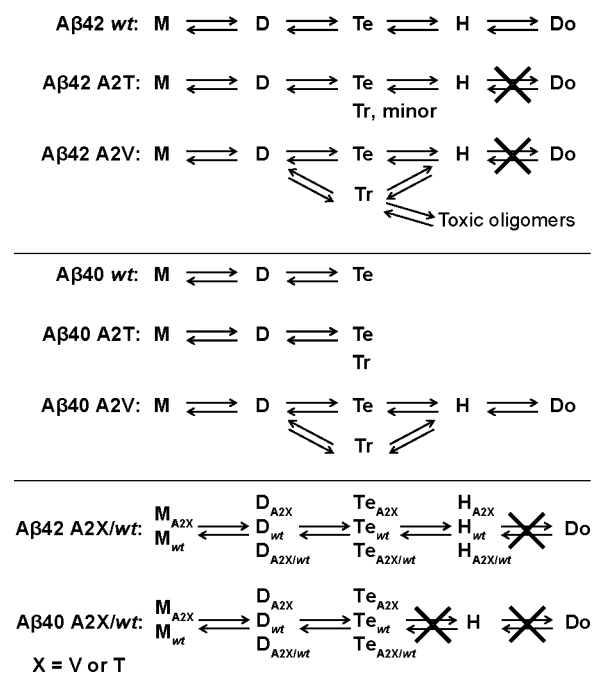


Figure 6. Different oligomerization patterns for wt A β , A2T and A2V alloforms, and mixtures. M, D, Tr, Te, H, and Do represent monomer, dimer, trimer, tetramer, hexamer, and dodecamer, respectively.

Iceland mutation A2T was observed to prevent the formation of A β 42 dodecamer, which was previously identified as an important neurotoxin in AD.^{8,9} These results are consistent with previous studies demonstrating that A2T is a protective mutation.³¹ However, our ion mobility studies show that the A2T mutation does not have a significant effect on oligomerization of the less toxic A β 40 isoform.

The A2V mutation was observed to inhibit the formation of A β 42 dodecamer as well. However, the A2V mutation leads to a much greater fraction of A β 42 trimer formation and observation of a unique $z/n = -8/3$ trimer peak that contains a significant fraction of hexamer not formed in A2T or wt A β 42. This result implies that A2V A β 42 may adopt another early assembly pathway through trimer that leads to toxic oligomers before going on to form fibrils. Even more interestingly, the A2V mutation shows significant effects on A β 40 assembly, resulting in the formation of A β 40 hexamer and dodecamer, which are not observed for A2T or wt A β 40. Hence, the A2V mutation changes the A β 40 aggregation pathway into a A β 42-like pathway, which is consistent with a previous ThT fluorescence study showing that A2V has a shorter aggregation lag phase than that of wt A β 40.³⁴ Although the relative intensity of dodecamer in A2V A β 40 is smaller than that for wt A β 42 (Figure 1f), this peptide is 10 times more abundant than A β 42 *in vivo*; hence, the fact that it produces potentially toxic oligomer states will be strongly amplified *in vivo*. This result, while not proof, is entirely consistent with the fact the A2V mutant results in early onset AD in homozygous carriers.³²

The effects of the A2T and A2V substitutions on wt A β 42 oligomerization were evaluated by coincubating equimolar

mixtures of the mutant and wt $A\beta$ 42 proteins. Both mutants formed small hetero-oligomers with wt $A\beta$ 42, including dimers, tetramers, and hexamers. However, no hetero- or homododecamers were observed, indicating that the formation of $A\beta$ 42 dodecamer is inhibited by the mutants. Co-incubation of A2T and wt $A\beta$ 40 shows formation of dimers and tetramers, which is similar to that of wt $A\beta$ 40, indicating no enhancement of aggregation by A2T (Figure S5). However, coincubation of A2V and wt $A\beta$ 40 shows only homo- and heterodimer and tetramer formation, indicating that hexamer and dodecamer formation is inhibited (Figure S6). This indicates that rapid A2V aggregation is inhibited by wt $A\beta$ 40. These results are consistent with previous studies suggesting that A2T protects against AD and that A2V heterozygous carriers are not affected by this mutation.^{31,32}

The N-terminus of $A\beta$ is relatively hydrophilic and appears to exist in a disordered state. It thus has been argued that it plays only a modest (or no) role in controlling $A\beta$ assembly compared to that of the central hydrophobic cluster region or the C-terminus.²⁴ However, we find here that single A2T and A2V amino acid substitutions do affect $A\beta$ oligomerization quite significantly, offering a mechanistic explanation for the phenotypes of humans expressing the cognate genes.

Threonine (T) and valine (V) have similar sizes but different hydrophobicities. The substitution of the neutral alanine (A) with a nucleophilic threonine or a hydrophobic valine will change the hydrophobicity of the N-terminus region and perhaps change the conformation of $A\beta$. A recent simulation study of A2T and A2V $A\beta$ 42 showed significantly different conformational landscapes of the $A\beta$ 42 monomer.⁴³ The A2T $A\beta$ 42 mutant makes the N-terminus more polar, which displays unusual long-range electrostatic interactions with residues such as Lys16 and Glu22.⁴³ Through such electrostatic interactions, the hairpin structure in the central hydrophobic region is disrupted, resulting in a population of unique conformations with only a C-terminal hairpin. In contrast, A2V $A\beta$ 42 shows an enhanced double-hairpin population due to hydrophobic interactions between the N-terminus and distant hydrophobic regions (central hydrophobic core and C-terminus hydrophobic region).⁴³ A previous simulation showed that the A2V mutation reduced the intrinsic disorder and increased the hairpin population in the $A\beta$ (1–28) monomer.⁴⁴ In addition, a previous MD simulation study showed that the N-terminus of $A\beta$ 40 displayed a β -strand structure at Ala-2-Phe-4, which was not present in $A\beta$ 42.⁴⁵ The hydrophilic N-termini of $A\beta$ proteins are on the surface of the oligomers; thus, the presence of an N-terminal β -strand in $A\beta$ 40 might prevent the hydrophobic core of the oligomers from adding additional $A\beta$ 40 molecules to form larger oligomers, which explains why $A\beta$ 40 aggregates slower and forms smaller oligomers than $A\beta$ 42. Therefore, the substitution of Ala with a hydrophobic Val may disrupt the formation of a hydrophilic N-terminal β -strand and make the hydrophobic core accessible for other $A\beta$ 40 molecules, shifting the A2V $A\beta$ 40 oligomerization toward those of $A\beta$ 42. Our ion mobility studies reveal different oligomerization for $A\beta$ proteins with a single mutation in the N-terminus region and imply the importance of the N-terminus region for $A\beta$ assembly, results consistent with previous studies.^{43–45}

In this work, we have demonstrated that IMS-MS is becoming a powerful tool to carry out studies that lead to understanding AD familial mutations. This is of significance, as single mutations have been implied to be important in disease

etiology. For instance, the G127V mutation in a prion variant has been shown recently to completely protect transgenic mice from prion disease.⁴⁶ Hence, understanding the mechanism of these positive substitutions becomes important for future therapeutic development. Thus, IMS-MS can be used as a new tool to study other systems of this kind and provide an insight into their structure–disease relationship.

CONCLUSIONS

(1) The A2T mutation prevents formation of $A\beta$ 42 dodecamer both in homo- and heterozygotes. The dodecamer has been implicated as a proximate toxic agent in AD. (2) The A2V mutation in homozygotes also prevents dodecamer formation in $A\beta$ 42 but promotes trimer formation, which may initiate a new pathway for early oligomer formation in $A\beta$ 42. (3) The A2V mutation in homozygotes promotes hexamer and dodecamer formation in $A\beta$ 40, whereas wt $A\beta$ 40 assembly terminates at the tetramer. Since $A\beta$ 40 is 10 times more prevalent than $A\beta$ 42 *in vivo*, facilitation of $A\beta$ 40 hexamer and dodecamer formation may well explain why the A2V mutation causes early onset AD in homozygotes. (4) Both the A2T and A2V mutations eliminate dodecamer formation in heterotypic mixtures with wt $A\beta$ 40 and $A\beta$ 42, consistent with the protective effects of these substitutions in heterozygotes. (5) Ion mobility methods are emerging as an important new tool in developing an understanding of the effect of familial mutations on $A\beta$ assembly in AD and the assembly of other mutated protein systems.

METHODS

Peptide and Sample Preparation. Full-length $A\beta$ and mutants were synthesized by N-9-fluorenylmethoxycarbonyl (Fmoc) chemistry.⁴⁷ The peptides were purified by reverse-phase HPLC, and their quality was validated by mass spectrometry and amino acid analysis. Samples were prepared in 10 mM ammonium acetate buffer, pH 7.4, at a final peptide concentration of 10 μ M. Equimolar mixtures of wt and mutant $A\beta$ were prepared at a total peptide concentration of 10 μ M (5 μ M of each peptide).

Mass Spectrometry and Ion Mobility Spectrometry Analysis. Most data were recorded on a home-built ion mobility spectrometry-mass spectrometer⁴⁸ or a Micromass QTOF2 quadrupole/time-of-flight tandem mass spectrometer. The home-built instrument is composed of a nanoelectrospray ionization (nano-ESI) source, an ion funnel, a temperature-controlled drift cell, and a quadrupole mass filter followed by an electron multiplier for ion detection.

Briefly, for ion mobility measurements, ions are generated continuously by a nano-ESI source, focused, and stored in the ion funnel. A pulse of ions is injected into a temperature-controlled drift cell filled with 3–5 Torr helium gas, where they gently pass through under the influence of a weak electric field. The injection energy can be varied from \sim 20 to \sim 150 eV. At low injection energy, the ions are rapidly thermalized by cooling collisions with the helium gas in the drift cell. At high injection energy, the ions are given energy that can lead to internal excitation before reaching thermal equilibrium. Such internal excitation can cause isomerization into a low energy structure or dissociation of large noncovalent complexes into small species.³⁷ Usually, the injection energy is kept as low as possible to minimize thermal heating of the ions during the injection process. (The injection energy studies are provided in the Supporting Information, Figures S1 and S2.) The ions exiting the drift cell are mass analyzed with a quadrupole mass filter and detected by a conversion dynode and channel electron multiplier, allowing a mass spectrum to be obtained.

The pulse of ions into the drift cell starts a clock at $t = 0$ and ends at $t = t_A$ when the ions reach the detector. This allows an arrival time distribution (ATD) to be obtained. The ATD can be related to the time the ions spend in the drift cell, which is directly related to the ion

mobility and collision cross section of the analyte ion.⁴⁹ The width of the ATD can be compared to the width calculated for a single analyte ion structure,⁴⁹ which gives information on the structural distribution favored in the ATD.

Transmission Electron Microscopy (TEM). Microscopic analysis was performed using a FEI T-20 transmission electron microscope operating at 200 kV. The A β samples were prepared using the same procedure as that for the mass spectrometry analysis. The samples were incubated at room temperature for 5 days. For TEM measurements, 10 μ L aliquots of samples were spotted on glow-discharged, carbon-coated copper grids (Ted Pella, Inc.). The samples were stained with 10 mM sodium metatungstate for 10 min and gently rinsed twice with deionized water. The sample grids were then dried at room temperature before TEM analysis.

■ ASSOCIATED CONTENT

● Supporting Information

The Supporting Information is available free of charge on the ACS Publications website at DOI: 10.1021/acscemneuro.5b00171.

Additional IMS-MS data of injection energy studies for A2T and A2V proteins, discussion of peak assignment for possible pentamer for A2V A β 42, ATDs of $z/n = -2$ for the A2T/wt and A2V/wt A β 42 mixtures, IMS-MS data of mixtures of A2T or A2V and wt A β 0, summary of ATDs and cross sections for A2T and A2V A β proteins, and TEM images for A β 40 and A β 42 proteins (PDF).

■ AUTHOR INFORMATION

Corresponding Author

*E-mail: bowers@chem.ucsb.edu; Tel.: 805-893-2893; Fax: 805-893-8703.

Author Contributions

X.Z. and M.T.B. designed research; X.Z., D.L., and R.R. performed research; X.Z. and M.T.B. analyzed data; X.Z., D.B.T., and M.T.B. wrote the paper.

Funding

The work was supported by National Institutes of Health grant nos. AG047116 (to M.T.B.) and AG041295 (to D.B.T.). The Material Research Laboratory Shared Experimental Facilities are supported by the MRSEC Program of the NSF under award no. DMR 1121053 (a member of the NSF-funded Materials Research Facilities Network, www.mrnf.org).

Notes

The authors declare no competing financial interest.

■ ACKNOWLEDGMENTS

We thank Margaret Condron at UCLA for synthesizing and purifying the A β proteins used in this work and the mass spectrometry facility in the Department of Chemistry and Biochemistry at UCSB.

■ ABBREVIATIONS

FAD, familial Alzheimer's disease; A β , amyloid β -protein; IMS-MS, ion mobility spectrometry-mass spectrometry; ATD, arrival time distribution

■ REFERENCES

(1) Mattson, M. P. (2004) Pathways towards and away from Alzheimer's disease. *Nature* 430, 631–639.
(2) Selkoe, D. J. (2001) Alzheimer's disease: Genes, proteins, and therapy. *Physiol. Rev.* 81, 741–766.

(3) Jakob-Roetne, R., and Jacobsen, H. (2009) Alzheimer's disease: From pathology to therapeutic approaches. *Angew. Chem., Int. Ed.* 48, 3030–3059.

(4) Teplow, D. (2013) On the subject of rigor in the study of amyloid β -protein assembly. *Alzheimer's Res. Ther.* 5, 39.

(5) Hayden, E., and Teplow, D. (2013) Amyloid β -protein oligomers and Alzheimer's disease. *Alzheimer's Res. Ther.* 5, 60.

(6) Bitan, G., Kirkitadze, M. D., Lomakin, A., Vollers, S. S., Benedek, G. B., and Teplow, D. B. (2003) Amyloid β -protein (A β) assembly: A β 40 and A β 42 oligomerize through distinct pathways. *Proc. Natl. Acad. Sci. U. S. A.* 100, 330–335.

(7) Bernstein, S. L., Dupuis, N. F., Lazo, N. D., Wyttenbach, T., Condron, M. M., Bitan, G., Teplow, D. B., Shea, J.-E., Ruotolo, B. T., Robinson, C. V., et al. (2009) Amyloid- β protein oligomerization and the importance of tetramers and dodecamers in the aetiology of Alzheimer's disease. *Nat. Chem.* 1, 326–331.

(8) Lesné, S., Koh, M. T., Kotilinek, L., Kaye, R., Glabe, C. G., Yang, A., Gallagher, M., and Ashe, K. H. (2006) A specific amyloid- β protein assembly in the brain impairs memory. *Nature* 440, 352–357.

(9) Gong, Y., Chang, L., Viola, K. L., Lacor, P. N., Lambert, M. P., Finch, C. E., Krafft, G. A., and Klein, W. L. (2003) Alzheimer's disease-affected brain: presence of oligomeric A β ligands (ADDLs) suggests a molecular basis for reversible memory loss. *Proc. Natl. Acad. Sci. U. S. A.* 100, 10417–10422.

(10) Kang, J., Lemaire, H.-G., Unterbeck, A., Salbaum, J. M., Masters, C. L., Grzeschik, K.-H., Multhaup, G., Beyreuther, K., and Muller-Hill, B. (1987) The precursor of Alzheimer's disease amyloid A4 protein resembles a cell-surface receptor. *Nature* 325, 733–736.

(11) O'Brien, R. J., and Wong, P. C. (2011) Amyloid precursor protein processing and Alzheimer's disease. *Annu. Rev. Neurosci.* 34, 185–204.

(12) Sherrington, R., Rogaev, E. I., Liang, Y., Rogaeva, E. A., Levesque, G., Ikeda, M., Chi, H., Lin, C., Li, G., Holman, K., et al. (1995) Cloning of a gene bearing missense mutations in early-onset familial Alzheimer's disease. *Nature* 375, 754–760.

(13) Borchelt, D. R., Thinakaran, G., Eckman, C. B., Lee, M. K., Davenport, F., Ratovitsky, T., Prada, C.-M., Kim, G., Seekins, S., Yager, D., et al. (1996) Familial Alzheimer's disease-linked presenilin 1 variants elevate A β 1–42/1–40 ratio in vitro and in vivo. *Neuron* 17, 1005–1013.

(14) Levy-Lahad, E., Wasco, W., Poorkaj, P., Romano, D., Oshima, J., Pettingell, W., Yu, C., Jondro, P., Schmidt, S., Wang, K., et al. (1995) Candidate gene for the chromosome 1 familial Alzheimer's disease locus. *Science* 269, 973–977.

(15) Tanzi, R. E., and Bertram, L. (2005) Twenty years of the Alzheimer's disease amyloid hypothesis: A genetic perspective. *Cell* 120, 545–555.

(16) Hendriks, L., van Duijn, C. M., Cras, P., Cruts, M., Van Hul, W., van Harskamp, F., Warren, A., McInnis, M. G., Antonarakis, S. E., Martin, J.-J., et al. (1992) Presenile dementia and cerebral haemorrhage linked to a mutation at codon 692 of the β -amyloid precursor protein gene. *Nat. Genet.* 1, 218–221.

(17) Nilsberth, C., Westlind-Danielsson, A., Eckman, C. B., Condron, M. M., Axelman, K., Forsell, C., Stenh, C., Luthman, J., Teplow, D. B., Younkin, S. G., et al. (2001) The 'Arctic' APP mutation (E693G) causes Alzheimer's disease by enhanced A β protofibril formation. *Nat. Neurosci.* 4, 887–893.

(18) Levy, E., Carman, M., Fernandez-Madrid, I., Power, M., Lieberburg, I., van Duinen, S., Bots, G., Luyendijk, W., and Frangione, B. (1990) Mutation of the Alzheimer's disease amyloid gene in hereditary cerebral hemorrhage, Dutch type. *Science* 248, 1124–1126.

(19) Tomiyama, T., Nagata, T., Shimada, H., Teraoka, R., Fukushima, A., Kanemitsu, H., Takuma, H., Kuwano, R., Imagawa, M., Ataka, S., et al. (2008) A new amyloid β variant favoring oligomerization in Alzheimer's-type dementia. *Ann. Neurol.* 63, 377–387.

(20) Miravalle, L., Tokuda, T., Chiarle, R., Giaccone, G., Bugiani, O., Tagliavini, F., Frangione, B., and Ghiso, J. (2000) Substitutions at codon 22 of Alzheimer's A β peptide induce diverse conformational

changes and apoptotic effects in human cerebral endothelial cells. *J. Biol. Chem.* 275, 27110–27116.

(21) Grabowski, T. J., Cho, H. S., Vonsattel, J. P. G., Rebeck, G. W., and Greenberg, S. M. (2001) Novel amyloid precursor protein mutation in an Iowa family with dementia and severe cerebral amyloid angiopathy. *Ann. Neurol.* 49, 697–705.

(22) Baumketner, A., Bernstein, S. L., Wyttenbach, T., Lazo, N. D., Teplow, D. B., Bowers, M. T., and Shea, J.-E. (2006) Structure of the 21–30 fragment of amyloid β -protein. *Protein Sci.* 15, 1239–1247.

(23) Krone, M. G., Baumketner, A., Bernstein, S. L., Wyttenbach, T., Lazo, N. D., Teplow, D. B., Bowers, M. T., and Shea, J.-E. (2008) Effects of familial Alzheimer's disease mutations on the folding nucleation of the amyloid β -protein. *J. Mol. Biol.* 381, 221–228.

(24) Sgourakis, N. G., Yan, Y., McCallum, S. A., Wang, C., and Garcia, A. E. (2007) The Alzheimer's peptides A β 40 and 42 adopt distinct conformations in water: A combined MD/NMR study. *J. Mol. Biol.* 368, 1448–1457.

(25) Takeda, T., and Klimov, D. K. (2009) Probing the effect of amino-terminal truncation for A β 1–40 peptides. *J. Phys. Chem. B* 113, 6692–6702.

(26) Hori, Y., Hashimoto, T., Wakutani, Y., Urakami, K., Nakashima, K., Condrón, M. M., Tsubuki, S., Saido, T. C., Teplow, D. B., and Iwatsubo, T. (2007) The tottori (D7N) and english (H6R) familial Alzheimer disease mutations accelerate A β fibril formation without increasing protofibril formation. *J. Biol. Chem.* 282, 4916–4923.

(27) Ono, K., Condrón, M. M., and Teplow, D. B. (2010) Effects of the english (H6R) and tottori (D7N) familial Alzheimer disease mutations on amyloid β -protein assembly and toxicity. *J. Biol. Chem.* 285, 23186–23197.

(28) Wakutani, Y., Watanabe, K., Adachi, Y., Wada-Isoe, K., Urakami, K., Ninomiya, H., Saido, T. C., Hashimoto, T., Iwatsubo, T., and Nakashima, K. (2004) Novel amyloid precursor protein gene missense mutation (D678N) in probable familial Alzheimer's disease. *J. Neurol., Neurosurg. Psychiatry* 75, 1039–1042.

(29) Gessel, M. M., Bernstein, S., Kemper, M., Teplow, D. B., and Bowers, M. T. (2012) Familial Alzheimer's disease mutations differentially alter amyloid β -protein oligomerization. *ACS Chem. Neurosci.* 3, 909–918.

(30) Chen, W.-T., Hong, C.-J., Lin, Y.-T., Chang, W.-H., Huang, H.-T., Liao, J.-Y., Chang, Y.-J., Hsieh, Y.-F., Cheng, C.-Y., Liu, H.-C., et al. (2012) Amyloid-Beta (A β) D7H mutation increases oligomeric A β 42 and alters properties of A β -zinc/copper assemblies. *PLoS One* 7, e35807.

(31) Jonsson, T., Atwal, J. K., Steinberg, S., Snaedal, J., Jonsson, P. V., Björnsson, S., Stefansson, H., Sulem, P., Gudbjartsson, D., Maloney, J., et al. (2012) A mutation in APP protects against Alzheimer's disease and age-related cognitive decline. *Nature* 488, 96–99.

(32) Di Fede, G., Catania, M., Morbin, M., Rossi, G., Suardi, S., Mazzoleni, G., Merlin, M., Giovagnoli, A. R., Prioni, S., Erbetta, et al. (2009) A recessive mutation in the APP gene with dominant-negative effect on amyloidogenesis. *Science* 323, 1473–1477.

(33) Messa, M., Colombo, L., del Favero, E., Cantù, L., Stoilova, T., Cagnotto, A., Rossi, A., Morbin, M., Di Fede, G., Tagliavini, F., et al. (2014) The peculiar role of the A2V mutation in amyloid- β (A β) 1–42 molecular assembly. *J. Biol. Chem.* 289, 24143–24152.

(34) Benilova, I., Gallardo, R., Ungureanu, A.-A., Castillo Cano, V., Snellinx, A., Ramakers, M., Bartic, C., Rousseau, F., Schymkowitz, J., and De Strooper, B. (2014) The Alzheimer disease protective mutation A2T modulates kinetic and thermodynamic properties of amyloid- β (A β) aggregation. *J. Biol. Chem.* 289, 30977–30989.

(35) Maloney, J. A., Bainbridge, T., Gustafson, A., Zhang, S., Kyauk, R., Steiner, P., van der Brug, M., Liu, Y., Ernst, J. A., Watts, R. J., et al. (2014) Molecular mechanisms of Alzheimer disease protection by the A673T allele of amyloid precursor protein. *J. Biol. Chem.* 289, 30990–31000.

(36) Wyttenbach, T., and Bowers, M. T. (2003) Gas-phase conformations: The ion mobility/ion chromatography method, in *Modern Mass Spectrometry* (Schalley, C., Ed.) pp 207–232, Springer, Berlin.

(37) Bernstein, S. L., Wyttenbach, T., Baumketner, A., Shea, J.-E., Bitan, G., Teplow, D. B., and Bowers, M. T. (2005) Amyloid β -protein: Monomer structure and early aggregation states of A β 42 and its Pro19 alloform. *J. Am. Chem. Soc.* 127, 2075–2084.

(38) Gessel, M. M., Wu, C., Li, H., Bitan, G., Shea, J.-E., and Bowers, M. T. (2012) A β (39–42) modulates A β oligomerization but not fibril formation. *Biochemistry* 51, 108–117.

(39) Lee, S., Zheng, X., Krishnamoorthy, J., Savelieff, M. G., Park, H. M., Brender, J. R., Kim, J. H., Derrick, J. S., Kochi, A., Lee, H. J., et al. (2014) Rational design of a structural framework with potential use to develop chemical reagents that target and modulate multiple facets of Alzheimer's disease. *J. Am. Chem. Soc.* 136, 299–310.

(40) Zheng, X., Gessel, M. M., Wisniewski, M. L., Viswanathan, K., Wright, D. L., Bahr, B. A., and Bowers, M. T. (2012) Z-Phe-Ala-diazomethylketone (PADK) disrupts and remodels early oligomer states of the Alzheimer disease A β 42 protein. *J. Biol. Chem.* 287, 6084–6088.

(41) Roychaudhuri, R., Lomakin, A., Bernstein, S., Zheng, X., Condrón, M. M., Benedek, G. B., Bowers, M., and Teplow, D. B. (2014) Gly25-Ser26 amyloid β -protein structural isomorphs produce distinct A β 42 conformational dynamics and assembly characteristics. *J. Mol. Biol.* 426, 2422–2441.

(42) Zheng, X., Liu, D., Klärner, F.-G., Schrader, T., Bitan, G., and Bowers, M. T. (2015) Amyloid β -protein assembly: The effect of molecular tweezers CLR01 and CLR03. *J. Phys. Chem. B* 119, 4831–4841.

(43) Das, P., Murray, B., and Belfort, G. (2015) Alzheimer's protective A2T mutation changes the conformational landscape of the A β 1–42 monomer differently than does the A2V mutation. *Biophys. J.* 108, 738–747.

(44) Nguyen, P. H., Tarus, B., and Derreumaux, P. (2014) Familial Alzheimer A2V mutation reduces the intrinsic disorder and completely changes the free energy landscape of the A β 1–28 monomer. *J. Phys. Chem. B* 118, 501–510.

(45) Urbanc, B., Cruz, L., Yun, S., Buldyrev, S. V., Bitan, G., Teplow, D. B., and Stanley, H. E. (2004) In silico study of amyloid β -protein folding and oligomerization. *Proc. Natl. Acad. Sci. U. S. A.* 101, 17345–17350.

(46) Asante, E. A., Smidak, M., Grimshaw, A., Houghton, R., Tomlinson, A., Jeelani, A., Jakubcova, T., Hamdan, S., Richard-Londt, A., and Linehan, J. M. (2015) A naturally occurring variant of the human prion protein completely prevents prion disease. *Nature* 522, 478–481.

(47) Lomakin, A., Chung, D. S., Benedek, G. B., Kirschner, D. A., and Teplow, D. B. (1996) On the nucleation and growth of amyloid β -protein fibrils: Detection of nuclei and quantitation of rate constants. *Proc. Natl. Acad. Sci. U. S. A.* 93, 1125–1129.

(48) Wyttenbach, T., Kemper, P. R., and Bowers, M. T. (2001) Design of a new electrospray ion mobility mass spectrometer. *Int. J. Mass Spectrom.* 212, 13–23.

(49) Mason, E. A., and McDaniel, E. W. (2005) Kinetic theory of mobility and diffusion: Sections 5.1–5.2, in *Transport Properties of Ions in Gases*, pp 137–193, Wiley-VCH, New York.